

A New Formulation for Hybrid LES-RANS Computations

Stephen Woodruff*

Ideally, a hybrid LES-RANS computation would employ LES only where necessary to make up for the failure of the RANS model to provide sufficient accuracy or to provide time-dependent information. Current approaches are fairly restrictive in the placement of LES and RANS regions; an LES-RANS transition in a boundary layer, for example, yields an unphysical log-layer shift. A hybrid computation is formulated here to allow greater control over the placement of LES and RANS regions and the transitions between them. The concept of model invariance is introduced, which provides a basis for interpreting hybrid results within an LES-RANS transition zone. Consequences of imposing model invariance include the addition of terms to the governing equations that compensate for unphysical gradients created as the model changes between RANS and LES. Computational results illustrate the increased accuracy of the approach and its insensitivity to the location of the transition and to the blending function employed.

Nomenclature

LES	Large-Eddy Simulation
RANS	Reynolds-Averaged Navier-Stokes
DES	Detached-Eddy Simulation
SST	Shear-Stress Transport
DNS	Direct-Numerical Simulation
C_{DES}	Turbulence model constant
c_μ	Turbulence model constant
$F(\lambda)$	A general model invariant
f	A typical flow variable
h	Half channel height
k	Modelled turbulent kinetic energy
ℓ_H	Hybrid length scale
P	Turbulent kinetic energy production
p	Pressure
Re	Reynolds number
Re_τ	Reynolds number based on friction velocity ($Re_\tau = u^* h / \nu$)
S_{ij}	Symmetric part of velocity gradient tensor
\tilde{S}_{ij}	Model-invariant S_{ij}
s	Model sensitivity variable
t	Time, non-dimensionalized by h/u^*
u^*	Friction velocity ($u^* = \sqrt{\tau_w / \rho}$)
\mathbf{v}	Velocity vector, non-dimensionalized by friction velocity u^*
$\mathbf{x} = (x, y, z)$	Streamwise, normal and spanwise coordinates, non-dimensionalized by half-channel width
\mathbf{x}', t', ξ	Variables on constant- λ side of coordinate transformation
y^+	Normal coordinate in wall units ($y^+ = y Re_\tau$)
β^*	Turbulence model constant
γ	Turbulence model constant
Δ	Mesh size for turbulence model, $\Delta = (\Delta_x \Delta_y \Delta_z)^{1/3}$

*Stephen Woodruff, Computational Aerosciences Branch, NASA Langley Research Center

$\Delta_x, \Delta_y, \Delta_z$	Mesh sizes in the three coordinate directions
λ	Model blending parameter (function of \mathbf{x}, t)
ν	Kinematic molecular viscosity
ν_t	Kinematic turbulent eddy viscosity
ρ	Density
σ_k	Turbulence model constant
σ_ω	Turbulence model constant
τ_w	Shear stress at wall
ω	Modelled omega (inverse turbulence time scale)
$\tilde{\partial}_t$	Model-invariant time derivative
$\tilde{\nabla}$	Model-invariant gradient operator

I. Introduction

Hybrid LES-RANS turbulence computations are becoming increasingly popular as more powerful computing resources permit some practical problems to be solved partially, but not fully, by LES. From the beginning, however, it has been recognized (*e.g.* Travin et al.¹) that best results are achieved if the turbulent (in contrast to the mean) parts of the flow in the LES and RANS regions are essentially uncoupled. If an LES-RANS transition is placed in, say, the log layer of a wall-bounded shear flow,^{2,3} requiring the turbulent parts of the flow to be coupled across the transition, the results are poorer.

This example suggests that current hybrid practice is not effective in merging the RANS and LES portions of the flow field when complex flow physics takes place in the LES-RANS transition zone. Remedying this shortcoming would permit much more freedom in the placement of RANS and LES sub-domains in a computation, so that the more costly LES need only be performed where the RANS model is inadequate to capture the necessary physics.

Techniques proposed to better control the LES-RANS transition include adding fluctuations,^{4,5} introducing a second level of velocity-field filtering,⁶ tuning the relation between the degree of LES-RANS blending and the wall distance⁷ and placing the transition at a particular position in the shear layer.^{8,9} Adjustments to the RANS eddy viscosity to accommodate the transition to LES^{10,11} have also been proposed, as have models for commutation error¹² and a hybrid formulation based on the blending of RANS and LES filters.^{13–16} While each of these approaches has met with some success, the goal of a general scheme permitting arbitrary placement of LES-RANS transitions to meet the requirements of the flow physics with minimum computational cost remains elusive.

It is argued here that achieving this goal requires distinguishing physical variations in flow variables from variations in the flow variables that arise solely due to the space and time dependence of the parameter controlling the blending of the hybrid model. The governing partial-differential equations describe balances between physical variations, so only by isolating the physical variations from model-parameter variations can an accurate computation be carried out. A formulation for doing so is presented in this paper, along with approximations for the additional terms introduced and turbulent channel-flow results computed using the formulation.

The fundamental element of this formulation is the concept of a model invariant, a quantity whose value is the same regardless of where one is in the RANS to LES transition. If a prediction is to be independent of the LES/RANS mix, which is purely an artifact of the model, it must be based on model invariants. Model invariants provide the tool for distinguishing between physical variations and model variations.

In an earlier paper,¹⁷ a two-stage process for developing hybrid computations was outlined. In the first stage, a blended model is developed and validated. (Here, a blended model is understood to mean a model which contains a structural, or blending, parameter, λ , which controls the variation of the blended model from a RANS model to an LES model.) Validation is performed with λ constant in the flow domain, not because one wishes to perform practical computations this way, but because this provides an unambiguous test of the model: with no variations in λ , there is no confusion between physical variations and model variations.

In the second stage¹⁷ of the development of the hybrid computation, the blended model is applied to the flow problem, with the blending parameter (now a function of space and time) controlling which subdomains of the problem are solved with the RANS model and which are solved with the LES model.

The validation aspect of the first stage must involve model invariants—quantities that are independent of the blending parameter, because only such quantities can produce physical predictions that are independent of the non-physical blending parameter. Simply replacing the constant blending parameter of the first stage with a time- and space-dependent blending parameter for the second stage destroys model invariance and introduces unphysical gradients due to blending-parameter variations. However, if the variable blending parameter is implemented in terms of the coordinate transformation introduced in the earlier paper¹⁷ and described below, model invariance is preserved and the correct physical balances in the governing equations are maintained.

Recent work of Hamba¹⁸ provides a clear demonstration of the importance of accounting for variable- λ effects in hybrid computations. In that work, Hamba filters DNS channel-flow data with a filter width that varies from a large value near the walls (emulating RANS) to a small value near the channel centerline (emulating LES). Individual terms in the continuity and momentum equations are evaluated, and it is found that the spatial variation in filter width generates terms in the equations whose magnitudes are on a par with other terms in those equations. These new terms are the same as those generated by the coordinate transformation introduced here to maintain model invariance.

In the following section, the formulation will be outlined and it will be shown how the preservation of model invariance in a computation is critical to maintaining the physical meaning of the computed variables. Then, channel flow computations will be presented showing that the formulation yields accurate results even when the LES-RANS transition is in the log layer and that it permits the transition location and blending function to be altered without significantly affecting the physical results.

II. Model-Invariant Hybrid Computations

The present formulation is based on the continuous-modeling concept proposed by Speziale,¹⁹ in which the turbulence model is constructed so as to be valid throughout the range from RANS to LES. The use of such a model allows a gradual transition between RANS and LES domains while maintaining the accuracy of the computation. To make this process meaningful, however, it is necessary to understand exactly how to interpret results in transition regions.

Let a continuous model be controlled by a blending parameter λ ; the model is a RANS model when $\lambda = 0$, an LES model when $\lambda = 1$ and a mixture of the two when $0 < \lambda < 1$. No further constraints shall be placed on the model. Similarly, no assumptions will be made about how the blending parameter λ is determined in a given flow problem: it could be specified in advance, specified in terms of the flow variables or specified as part of an adaptive-grid scheme.

In the same spirit, no specific schemes of averaging or filtering will be defined for the RANS and LES variables. Instead, the decomposition of the flow variables into modelled and resolved components will be implied by the model. While it is common to define hybrid computations in term of averaging and filtering operations appropriate for RANS and LES and then develop a model, the absence of a systematic—much less rigorous—procedure for getting from the definition of an average to a model makes this approach problematic. Reversing the process eliminates the problem.

Model-invariant quantities provide the means to extract physical meaning from computed variables, regardless of where λ is in the range from zero to one. These are quantities that are at least approximately independent of the model blending parameter λ . One type of model-invariant quantity results from projecting computational variables into a subspace common to all forms of the model. An example is the mean of a flow variable such as the velocity. The RANS mean velocity at a point in a flow should correspond to the mean velocity from an LES computation at the same point. A second type of model-invariant quantity can involve flow quantities with representations in both the super-grid, resolved motion and in the sub-grid, modelled motion. The Reynolds stress tensor, for example, is composed of the resolved and modelled Reynolds stresses (plus, potentially, terms resulting from the interaction between resolved and modelled components). The modelled and resolved parts trade off as the mixture of LES and RANS models changes, allowing the total to remain constant. The same effect can result if the model invariant explicitly contains the blending parameter.

Model-invariant quantities permit connections to be made between flow variables computed with different mixtures of the RANS and LES models (different values of λ). Model invariants of the first type described above relate flow variables computed with some mixture of RANS and LES models to the corresponding RANS flow variables. Those of the second type yield relations between two sets of flow variables at arbitrary values of λ . These are most useful when the values of λ are close together and the filtering implicit in the

resolved/modelled decomposition implied by the blended model equations is negligible. In particular, letting one value of λ approach the other yields, in the limit, the differential relation $\frac{\partial F}{\partial \lambda} = 0$, where $F(\lambda)$ is some model invariant. This differential expression of model invariance plays a critical role in the present work.

The relationship between variables that is defined by a model invariant is clearly a special one and, in practice, such relationships may well be approximate. The accuracy of these model-invariant relationships is a property of the equations defining the blended model; one which might provide important guidance in the development of new hybrid models.

Any prediction of a blended-model computation that is to be independent of the non-physical blending parameter must ultimately be based on model invariants. This is the essential observation of the present hybrid formulation, and it has a number of important consequences that are outlined in the following subsections. Chief among these is that preservation of the differential model invariant as a flow evolves in time requires certain terms be added to the governing equations. This requirement is related to the fact that the interpretation of $\frac{\partial F}{\partial \lambda} = 0$ when λ is itself a function of space and time becomes murky. A coordinate transformation is introduced in the next subsection that clarifies this situation by relating the constant- λ and variable- λ cases in a precise way.

II.A. Coordinate Transformation

Attaching meaning to a hybrid computation for $0 < \lambda < 1$, but still with $\lambda = \text{const.}$, is simple: the model should yield model-invariant quantities that agree with experiment or other computations to the required degree of accuracy. Validation amounts to demonstrating that this is the case.

The standard means for extending a hybrid model to the $\lambda \neq \text{const.}$ case has been to replace the constant blending parameter λ with a time- and space-varying λ .²⁰ It will be argued below that this destroys model invariance and, with it, the means for extracting physically meaningful information from the computation. In contrast, in the present formulation the extension of the hybrid model to variable λ is based on a coordinate transformation between the $\lambda = \text{const.}$ case and the $\lambda \neq \text{const.}$ case. The advantage of this interpretation is that it guarantees that all properties of the blended model equations and their solutions that were validated for the $\lambda = \text{const.}$ case imply, via the coordinate transformation, equivalent properties for the model equations and their solutions in the $\lambda \neq \text{const.}$ case. In particular, quantities determined to be model invariant and used for model validation when $\lambda = \text{const.}$ will remain model invariant when $\lambda \neq \text{const.}$ This is not the case in the standard interpretation.

The effect of this alternative interpretation on the governing equations is to add terms involving the change in the flow variables due to a change in the blending parameter. These terms compensate for the spurious contributions to the flow-variable derivatives that arise from changes in the model structure, so the balance of physical quantities in the governing equations remains valid.

The transformation is introduced for a typical flow variable $f = f(t', \mathbf{x}', \xi)$, a function of space and time and of the model blending parameter ξ , which one wishes to set equal to $\lambda = \lambda(t', \mathbf{x}')$. Simply doing so, however, means that derivatives of f will have contributions both from the explicit dependence of f on t' and \mathbf{x}' and from the implicit dependence of f on t' and \mathbf{x}' through λ . This latter contribution is unphysical.

Instead, consider the coordinate transformation $t = t'$, $\mathbf{x} = \mathbf{x}'$, $s = \xi - \lambda(t', \mathbf{x}')$. The new variable s , which provides a means for describing variations with respect to model blending, is zero in the physical situation, yielding $\xi = \lambda$. Except for the introduction of s , this transformation amounts to the replacement of the constant λ by a variable λ that is characteristic of the standard interpretation of a hybrid LES-RANS computation. Where the present interpretation differs from the standard interpretation is in the consistent application of the transformation to the governing equations. In particular, spatial and temporal derivatives in the new (unprimed) coordinate system now have two contributions: the derivative with respect to the corresponding primed coordinate and a new contribution reflecting the change in λ . Thus, the time derivative transforms as

$$\frac{\partial}{\partial t'} = \tilde{\partial}_t \equiv \frac{\partial}{\partial t} - \frac{\partial \lambda}{\partial t} \frac{\partial}{\partial s} \quad (1)$$

the gradient operator becomes

$$\nabla' = \tilde{\nabla} \equiv \nabla - (\nabla \lambda) \frac{\partial}{\partial s} \quad (2)$$

(∇' is the gradient operator on the primed variables), the divergence of a vector \mathbf{v} becomes

$$\nabla' \cdot \mathbf{v} = \tilde{\nabla} \cdot \mathbf{v} \equiv \nabla \cdot \mathbf{v} - (\nabla \lambda) \cdot \frac{\partial \mathbf{v}}{\partial s} \quad (3)$$

and so on. (These expressions are understood to be evaluated at $s = 0$.) The new terms are equal and opposite to the spurious contributions from the introduction of the space- and time-dependent λ and serve to subtract out those contributions. Only the correct, physical, contributions to the derivatives of the flow variables remain and the physical balances in the governing equations are restored.

The operators introduced above are essentially equivalent to those of Germano,¹³ Hamba,^{6,18} Rajamani and Kim,¹⁴ and Sanchez-Rocha and Menon,^{15,16} because each addresses a specific type of the general blended model discussed here. The relationship between the present work and that of these authors is discussed further later on.

II.B. Preservation of Model Invariance.

The transformation formalism implies that model invariance is preserved when $\lambda \neq \text{const.}$ in a hybrid computation employing the proposed formulation, but not in one using the standard formulation. Any validation of the blended model, or its constituent RANS and LES models, is thus preserved in the proposed formulation when $\lambda \neq \text{const.}$ Validation of models in the standard formulation, on the other hand, becomes moot.

Under the coordinate transformation described above, derivatives with respect to the model blending parameter, ξ , in the $\lambda = \text{const.}$ case transform to derivatives with respect to s in the $\lambda \neq \text{const.}$ case. Since the model invariance of a quantity may be expressed as the condition that these derivatives are zero, the transformation shows that model invariance in the constant- λ case implies model invariance in the variable- λ case. Differentiating these conditions with respect to time yields the conclusion that time derivatives of model invariants are also model invariant in the variable- λ case. This implies model invariance is preserved as the flow evolves. If the derivatives are zero in the present interpretation, however, they cannot be zero in the standard interpretation, because they differ by the absent correction terms. Thus, model invariance is not preserved in the standard interpretation.

Validation and other conclusions drawn for the constant- λ case are invalid when $\lambda \neq \text{const.}$, due to the loss of model invariance. Validation, and, in general, the ability to extract physically meaningful information, is preserved in the present formulation when $\lambda \neq \text{const.}$, due to the preservation of model invariance.

II.C. Hybrid Model Equations

The non-dimensional incompressible Navier-Stokes equations may now be written for a model-invariant hybrid computation as

$$\begin{aligned}\tilde{\nabla} \cdot \mathbf{v} &= 0 \\ \tilde{\partial}_t \mathbf{v} + (\mathbf{v} \cdot \tilde{\nabla}) \mathbf{v} &= -\tilde{\nabla} p + \tilde{\nabla} \cdot \left[\left(\frac{1}{Re} + \nu_t \right) \tilde{\nabla} \mathbf{v} \right].\end{aligned}\quad (4)$$

In these equations, \mathbf{v} is the resolved-scale velocity, p is the resolved-scale pressure and ν_t is the eddy viscosity.

The basis for the hybrid model employed in this paper is Strelets' Detached-Eddy Simulation (DES) hybrid model,²¹ which is in turn based on Menter's SST model,²²

$$\begin{aligned}\tilde{\partial}_t k + (\mathbf{v} \cdot \tilde{\nabla}) k &= P - \frac{k^{3/2}}{\ell_H} + \tilde{\nabla} \cdot \left[\left(\frac{1}{Re} + \sigma_k \nu_t \right) \tilde{\nabla} k \right] \\ \tilde{\partial}_t \omega + (\mathbf{v} \cdot \tilde{\nabla}) \omega &= \frac{\gamma}{\nu_t} P - \beta \omega^2 + \tilde{\nabla} \cdot \left[\left(\frac{1}{Re} + \sigma_\omega \nu_t \right) \tilde{\nabla} \omega \right].\end{aligned}\quad (5)$$

The production P is expressed as $P = \nu_t \tilde{S}_{ij} \tilde{S}_{ij}$, where \tilde{S}_{ij} is the symmetric part of the tensor $\tilde{\nabla} \mathbf{v}$.

The length scale ℓ_H switches between the RANS and LES length scales and was defined by Strelets to be $\ell_H = \min(k^{1/2}/(\beta^* \omega), C_{DES} \Delta)$. The continuous modeling approach employed here calls for a smoother transition between the RANS and LES models, which suggests a definition like $\ell_H = (1 - \lambda)k^{1/2}/(\beta^* \omega) + \lambda C_{DES} \Delta$. However, the equations were found to be numerically better behaved if, instead of blending the RANS and LES length scales linearly, the dissipation term in the kinetic-energy equation is a linear blend of the RANS and LES dissipation expressions: $(1 - \lambda)\beta^* \omega k + \lambda k^{3/2}/(C_{DES} \Delta)$. The model constants, following Menter,²² are the standard $k - \omega$ values.

The Menter SST RANS model upon which the Strelets DES model is based employs an eddy viscosity ν_t which switches from the standard k/ω to an alternative form that is superior for adverse-pressure-gradient

flows. Since the channel-flow pressure gradient is never unfavorable, $\nu_t = k/\omega$ is always used in the present computation. Similarly, the Menter model blends a $k - \omega$ near-wall formulation with $k - \epsilon$ features away from the wall; these $k - \epsilon$ features were not implemented, so the present RANS model is essentially a $k - \omega$ model everywhere. This is appropriate for the present computation since the transition to LES would largely supercede any transition to the $k - \epsilon$ model.

II.D. Model Sensitivities

The new terms introduced into the governing equations to make them model invariant involve derivatives of the flow variables with respect to s , reflecting the sensitivities of the flow variables to variations in the model. These sensitivities may be determined in a variety of ways, including by solving additional transport equations found by differentiating the flow equations with respect to s and by evaluating finite-difference approximations in s -space.¹⁷

The approach to the determination of the model sensitivities employed here will be through the model-invariant quantities themselves. The differential model-invariant definition $\frac{\partial F}{\partial s} = 0$ is, when the differentiation with respect to s is carried out, an equation involving the s -derivatives of the flow variables from which F is constructed. A full set of these relations comprises a set of equations that may be solved to yield the model sensitivities. Repeated differentiation yields expressions for higher-order derivatives of the flow variables with respect to s .

In the computation performed in the following section, the sum of the resolved and modelled turbulent kinetic energies is chosen as an approximate model invariant, as is the dissipation expressed by the destruction term in the turbulent kinetic energy equation (because this term is the sink for all turbulent energy). The turbulent length scale $k^{1/2}/\omega$ is employed as a third invariant. These three invariants may be used to give the s derivatives of k , ω and the velocity magnitude. The velocity magnitude derivative is split into three component derivatives according to overall proportions determined by numerical experimentation and guided by the proportions seen in earlier work.¹⁷ This approximation to the model sensitivities is very crude but will be seen nevertheless to give good results.

A more sophisticated approximation would use components of the shear-stress tensor $u_i u_j - \nu_t S_{ij}$ to fix the velocity-component s derivatives and eliminate the need for the empirical proportionality factors. The inverse time scale ω itself might be used as a model invariant, instead of $k^{1/2}/\omega$, since it could be argued the turbulent time scale ought to be independent of the LES-RANS model mixture.

II.E. Comments

To summarize, a precise characterization of the computational variables inside an LES-RANS transition zone was sought, leading to the introduction of concepts of model invariance and model-invariant quantities as a means for extracting physically meaningful results. Maintaining model invariance in a computation was found to require adding terms to the governing differential equations that restore the physical balances lost when a time- and space-dependent blending parameter appears in the hybrid model.

The model-invariant hybrid computation has three principle ingredients: the overall formulation itself, the hybrid model and the approximation for the model sensitivities. Only the formulation is fundamental to the approach: the model and the approximation for the model sensitivities employed here are simple examples that work well for the turbulent channel computations of the following section, but there are many opportunities for improvement. In fact, this separation of the mathematics of handling the blending properly from the physical models should allow modeling research to focus on true physical differences between models, without being misled by spurious model-variation effects. The formulation also has the potential to clarify what the requirements for a good model are.

The value of a flow variable (like f , discussed above) at a point in space and time depends on the entire function λ and not just its value at that point. To assess fully the effect of λ on flow quantities requires the introduction of functional derivatives. The present development is predicated on the assumption that flow variables depend primarily on the local value of the blending function λ . This assumption seems drastic—and it is—but the assumption has already been made in our turbulence models. The Smagorinsky model, for example, is based entirely on the local value of the resolution, or grid constant, Δ . The same is true of the LES part of the Strelets DES model employed here. So it is certainly reasonable to at least consider employing the same approximation in the present hybrid formulation.

It is not too surprising that there are many cases where the standard interpretation of a hybrid LES-RANS computation gives good results, in spite of the foregoing discussion. If the LES-RANS transitions are placed, as recommended by DES practitioners,¹ so that RANS and LES turbulence is not coupled and so the physics in the transition regions is fairly benign, then the model sensitivities are likely to be fairly small and the correction terms in the governing equations are likely to be negligible.

In general, however, all dependent variables are subject to spurious variations that arise solely from variations in the blending parameter. The present formulation shows how to fix this problem.

III. Turbulent Channel Flow

Plane channel flow provides a natural test for the present approach, since it is recognized as presenting particular difficulties for hybrid computations. A series of tests of the model-invariant formulation will be presented in this section that show it to be more accurate than the standard formulation and that this accuracy is maintained through changes in the position and thickness of the transition zone and changes in the shape of the blending function.

III.A. Problem Definition

Let lengths be normalized by the half-channel height, velocities by the friction velocity $u^* = \tau_w / \rho$ (τ_w is the shear stress at the wall) and let ν be the molecular viscosity. The Reynolds number is $Re_\tau = hu^* / \nu$. The length and span of the channel are 2π and $4/3\pi$, respectively, and these directions are periodic. Constant volume flux is maintained by controlling the mean pressure gradient: at each time step, the nominal mean pressure gradient is augmented by a term proportional to the amount by which the specified volume flux exceeds the actual volume flux.

The LES-RANS transition regions are parallel to the walls, so the blending function is a function of y only. The blending function is specified in advance. In most of the computations, the blending function varies within the transition region according to a cubic spline function, which allows the first derivative of the blending function to be zero at the edges of the transition region. The maximum and minimum values of the blending function were chosen to be 0.1 and 0.9 (rather than 0 and 1) to facilitate a future comparison with results computed according to a scheme¹⁷ employing finite differences in s to give the model sensitivities.

Tests were conducted of the present approach with the RANS/LES transition located at various distances from the wall, with various transition thicknesses. Tests were conducted at $Re_\tau = 180$ and 395 and results compared with the direct-numerical simulation results of Moser, Kim and Mansour.²³

III.B. Numerics

The incompressible-flow equations are solved employing standard numerical techniques. The streamwise (x) and spanwise (z) directions are discretized spectrally; the nonlinear terms are handled pseudo-spectrally. The cross-channel direction (y) is discretized with fourth-order central finite differences on a uniform computational grid transformed from the non-uniform physical grid. The physical grid is composed of 80 gridpoints between the walls in the normal direction, with the grid point nearest the wall at $y^+ < 1$ for $Re_\tau = 180$ and at $y^+ = 1.5$ for $Re_\tau = 395$.

Time advancement is second-order accurate and employs a Newton iterative scheme, following that of Ref. 24. The relatively low Reynolds number of the present test cases allows satisfactory convergence and time-step size with only the molecular viscosity terms implemented in the approximate Jacobian of the Newton scheme. The velocity field resulting from the time advancement is constrained to satisfy the continuity equation at each time step.

No special treatment was required for solution of the momentum equations with the new source terms. Special treatment was required to satisfy the continuity equation, because it is no longer simply $\nabla \cdot \mathbf{v} = 0$. An iterative Poisson-solver scheme was found to be effective for solving the new form of the continuity equation with the additional model-invariance terms.

It was found in the course of performing the computations that some fairly aggressive measures had to be taken to prevent the turbulent kinetic energy from becoming negative. Interestingly, limited regions of negative turbulent kinetic energy were found to be supportable in a standard hybrid LES-RANS computation if the usual precautions were taken to ensure negative values did not contaminate the entire computation: care was taken that the square root of a negative number was not evaluated, etc. While certainly undesirable,

these excursions remained localized, relatively few in number and did not significantly affect the overall solution.

The addition of the model-invariance terms, however, permits low-kinetic-energy excursions to pass occasionally from the LES regions to RANS regions, where apparently this did not happen before. The RANS model equations eventually cause the computation to blow up, because, unlike the LES model, two-equation RANS models do not support a simultaneous balance between the production and destruction source terms in the kinetic energy and ω equations. (When k is small, the model equations are dominated by the source terms.)

To eliminate this problem, lower limits were imposed on the production and $S_{ij}S_{ij}$ in the model equations. Also, the kinetic-energy-equation update in the time-advancement algorithm was limited to positive values at any location where the kinetic energy falls below a specified fraction of the plane-averaged kinetic energy at the same distance from the wall. These measures were sufficient to eliminate the negative kinetic-energy excursions.

Since the focus of the present work is on the hybrid formulation, rather than on the specific hybrid model employed, this *ad hoc* fix to the problem of negative kinetic-energy excursions was deemed acceptable for the present computations. The underlying problem may appear in other hybrid computations, though, and designing new hybrid models that avoid negative-energy excursions entirely would clearly be desirable.

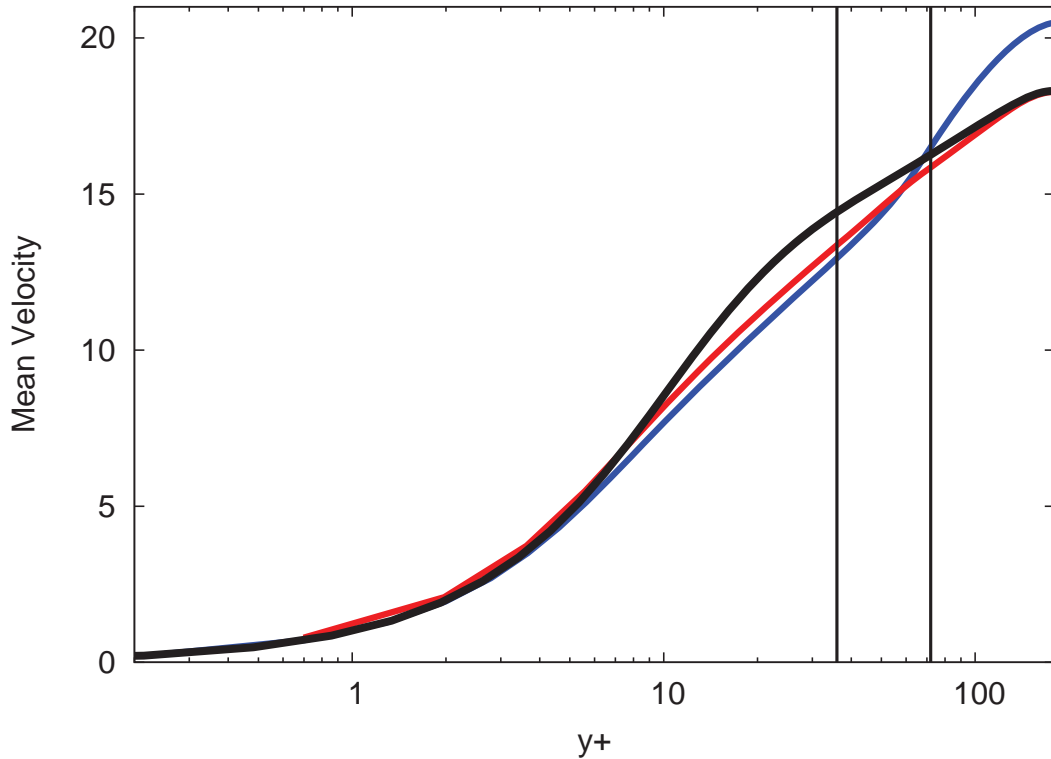


Figure 1. Mean-velocity profiles from model-invariant computation (red curve), standard hybrid computation (blue curve) and DNS of Moser, Kim and Mansour²³ (black curve) at $Re_\tau = 180$. Vertical lines indicate edges of transition zone.

III.C. Results

A hybrid computation for the channel-flow problem at $Re_\tau = 180$ was set up with spectral resolution in x and z of $N_x = N_z = 10$, coarse enough so that the computation could not support the near-wall streamwise vorticity required for turbulent-energy generation in an LES computation. The lower-wall transition between

RANS and LES is at $0.2 \leq y \leq 0.4$, corresponding to $36 \leq y^+ \leq 72$ and lies within the log layer. The upper-wall transition layer is positioned to make the configuration symmetric.

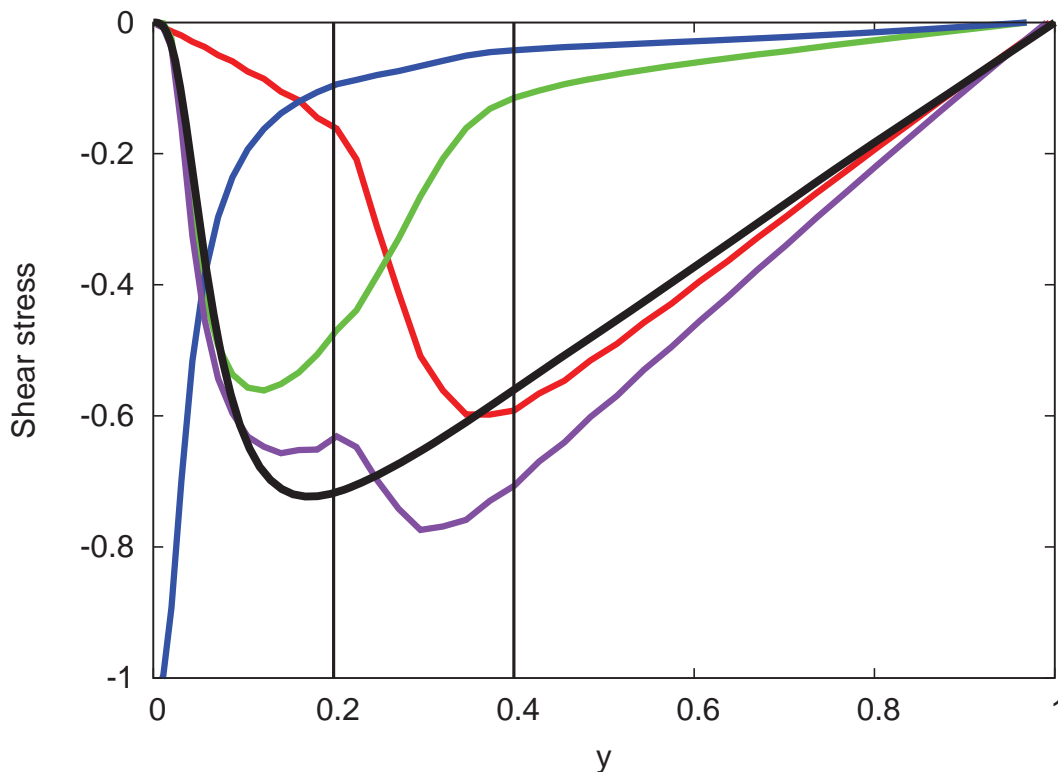


Figure 2. Shear-stress components from model-invariant computation at $Re_\tau = 180$: resolved turbulent stress (red curve), modeled turbulent stress (green curve), viscous stress (blue curve), total turbulent stress (purple curve), DNS²³ turbulent stress (black curve).

All profiles presented in this section are the result of spatial averaging over the $x - z$ plane and temporal averaging over a period of greater than 100 eddy turnover times (based on channel half width and maximum streamwise RMS fluctuating velocity).

The main point of this paper is illustrated in Figure 1, where the mean velocity profile for the model-invariant hybrid computation is compared with the DNS of Moser, Kim and Mansour²³ and with a standard hybrid computation performed with the same blended turbulence model but without the new terms for preserving model invariance.

As is typical of hybrid computations of this problem,^{2,3} the standard hybrid computation significantly over-predicts the velocity at the center of the channel. The model-invariant hybrid computation, on the other hand, fairly accurately fulfills the goals of the formulation: the solution matches the pure LES solution in the central, LES, portion of the channel, matches the pure RANS solution near the wall ($y^+ \leq 36$) and smoothly passes from one to the other in the transition region $36 \leq y^+ \leq 72$.

Further insight into the effect of the model-invariance correction terms may be gleaned from the profiles of the contributions to the shear stress. In Figure 2, the resolved Reynolds stress, modeled Reynolds stress, total Reynolds stress and viscous stress are shown. The total turbulent stress (sum of the modeled and resolved turbulent-stress contributions) agrees reasonably with the DNS turbulent shear stress. There is some over-prediction in the LES region, corresponding to an under-prediction in the RANS region. (The RANS discrepancy is likely due to the low Reynolds number of the flow, as well as to the use, noted earlier, of $\lambda = 0.1$ in the RANS region instead of $\lambda = 0$.)

Most significantly, the resolved contribution to the turbulent stress in Figure 2 has a higher peak than that of the corresponding standard hybrid computation (Figure 3). There is also less overlap between the

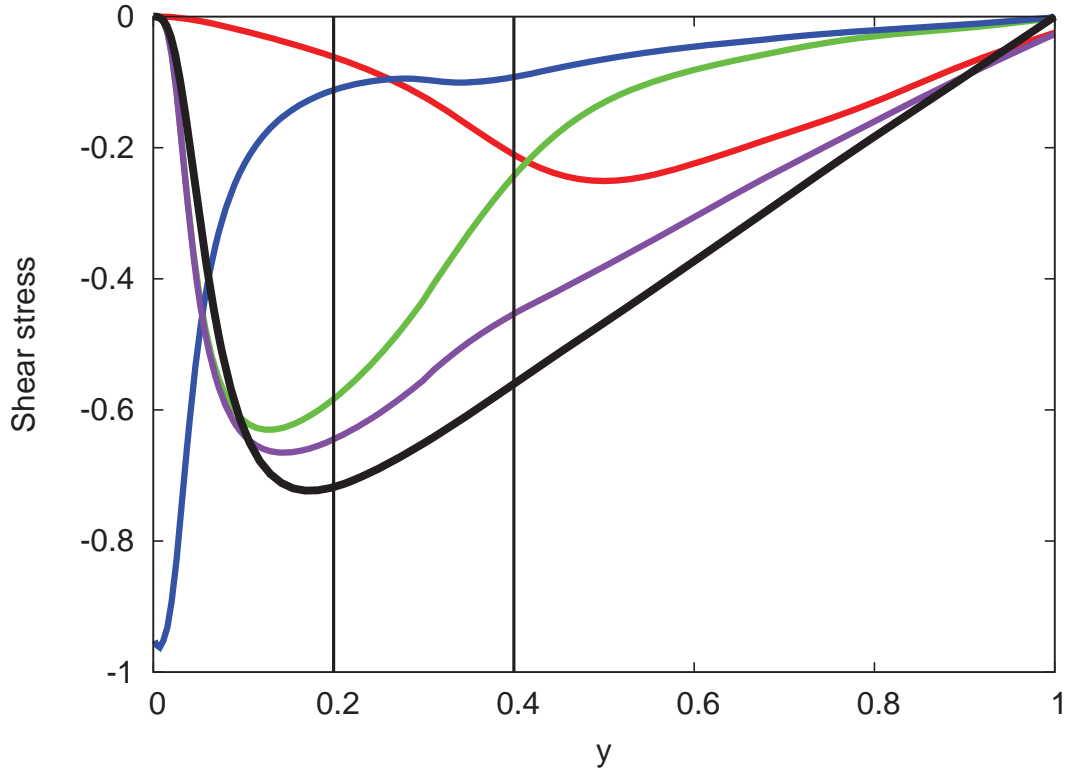


Figure 3. Shear-stress components from standard hybrid computation at $Re_\tau = 180$: resolved turbulent stress (red curve), modeled turbulent stress (green curve), viscous stress (blue curve), total turbulent stress (purple curve), DNS²³ turbulent stress (black curve).

modeled and resolved contributions in the model-invariant computation. This indicates the correction terms are helping to keep the modeled stress dominant in the RANS zone and the resolved Reynolds stress dominant in the LES zone, eliminating the “double-counting” of the shear stress that leads to the log-layer shift in standard hybrid computations.

The three normal resolved Reynolds stresses are shown in Figures 4, 5 and 6; while the results of the present method show some improvement in the LES regions, the well-known failure of Boussinesq-approximation RANS models to provide adequate predictions of the normal stresses makes the overall predictions fairly poor.

The insensitivity of the model-invariant computation to the position and thickness of the transition layer is demonstrated in Figure 7. The mean-flow velocity profiles from computations with a variety of transition layers (indicated by the vertical lines color-coded to the profiles) are seen to be very similar, indicating a fairly wide variation in both location and thickness is possible. The streamwise and spanwise resolutions were increased to $N_x = N_z = 12$ as the transition moved closer to the wall and decreased to $N_x = N_z = 8$ for the higher transitions.

The resolved shear stresses, on the other hand, should change with changes in the transition layer and this is seen in Figure 8. The well-defined jump in the shear stress from low RANS values to high LES values in the transition layer seen in Figure 2 is seen for these computations as well.

To evaluate the effect of varying the shape of the blending function in the transition region, computations were performed with $\lambda(y)$ varying linearly across the transition region and with $\lambda(y)$ varying as the hyperbolic-tangent function. The velocity-profile results in Figure 9 show little sensitivity to these changes in the shape of the blending function. The resolved shear stresses exhibited in Figure 10 are also largely insensitive to these changes, though the linear case deviates somewhat from the other two, most likely due

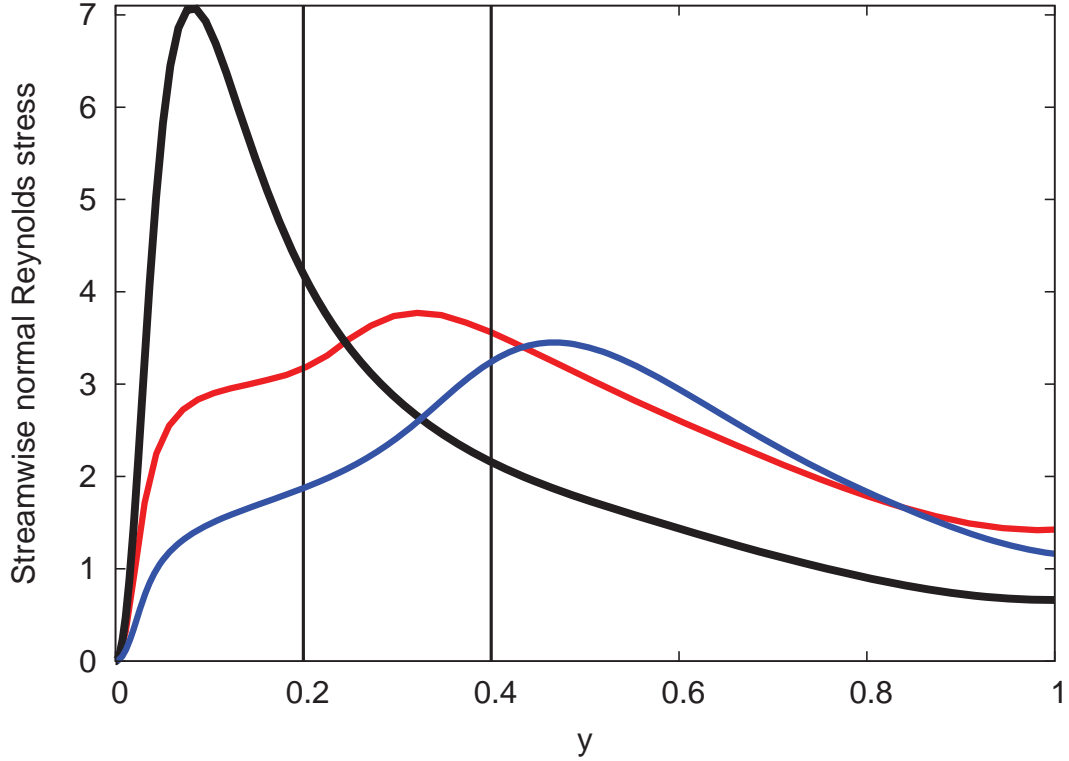


Figure 4. Normal resolved Reynolds-stress component from model-invariant computation (red curve), standard hybrid computation (blue curve) and DNS²³ (black curve) at $Re_\tau = 180$.

to the discontinuity in that blending-function's derivative at the transition-region edges. The shear-stress profile for the linear case also exhibits some waviness, seen to a small degree in some of the earlier figures. This appears to be evidence the numerics are on the verge of being pushed too far by the model-invariance terms.

Finally, Figures 11 and 12 show the mean velocity and shear-stress profiles with various transition-region locations and thicknesses at $Re_\tau = 395$, performed on the same grid as the earlier computations. As for the lower Reynolds number, agreement with the DNS data is consistently good as the height and thickness of the transition layers is varied.

IV. Discussion

The present formulation is sufficiently fundamental that earlier efforts to improve LES-RANS transitions may be understood in terms of its concepts. The filtering approach of Hamba,⁶ for example, may be viewed as a means of estimating the model sensitivities by comparing the results of filtering with slightly different filter widths. Hamba notes the relationship between his source terms (and, by extension, those of the present work) and the imposed stochastic forcing of Keating et al.⁴ It may further be remarked that the utility of the shear stress as the reference quantity in the feedback loop employed by Keating et al.⁴ to determine the stochastic forcing is due to its status as a model-independent quantity, in the sense defined here.

The work of Shur et al.⁷ improves log-layer behavior by a special selection of what is, in the present notation, λ , in terms of the distance from the wall. The selected λ seems to have the effect of reducing the magnitude of the present model-invariant source terms. For a given problem, one may always determine λ so as to minimize the source terms, but there is no guarantee that the λ so determined will be applicable to a wide range of flows. In a similar vein, the authors of Refs. 8 and 9 choose their transition locations (thus

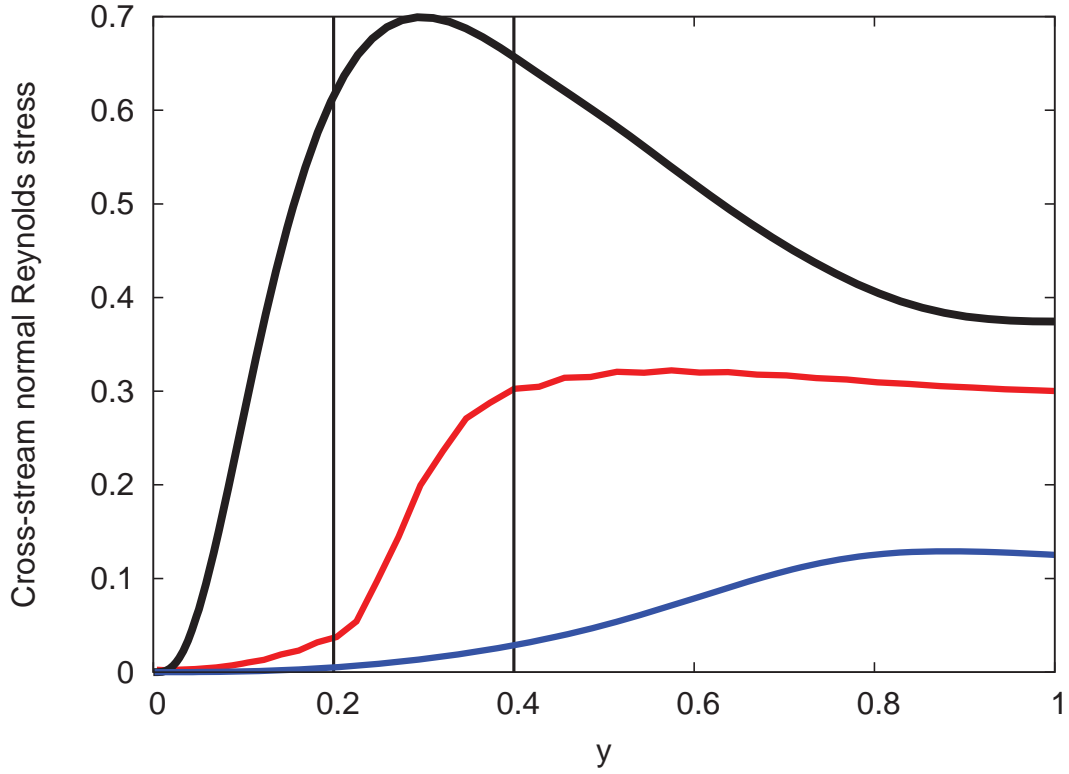


Figure 5. Normal resolved Reynolds-stress component from model-invariant computation (red curve), standard hybrid computation (blue curve) and DNS²³ (black curve) at $Re_\tau = 180$.

determining λ) so as to yield the most accurate results, suggesting that the source terms are minimized at these locations.

Wallin and Girimaji¹² also add source terms to their equations to account for the effect of variations in the blending parameter; these terms are modelled with eddy-viscosity expressions. Germano,¹³ Rajamani and Kim¹⁴ and Sanchez-Rocha and Menon^{15,16} have worked with blended models based on a linear combination of RANS and LES filters. They, too, add source terms to the flow equations, which are determined via inverse filtering¹⁴ or are modelled.¹⁶ As noted earlier, the characterization of the blended model in terms of filters was avoided in the present development specifically because it generates terms whose determination is problematic. In contrast, a variety of avenues are open for the estimation of the model sensitivities employed by the present approach.

Some of the analyses just mentioned lead to modified RANS eddy viscosities. Efforts specifically to modify the RANS eddy viscosity to accommodate the LES resolved stresses, such as those of Medic et al.¹⁰ and Breuer et al.,¹¹ perhaps bear the closest resemblance to the spirit of the present approach. Medic et al.,¹⁰ in particular, explicitly sought to establish a connection between RANS and LES viscosities in a hybrid computation, just as the present approach does more generally for all flow variables by means of model invariants.

It may also be noted that the well-known Germano identity,²⁵ employed in dynamic LES subgrid models, relates the Reynolds stress at different filter widths and so may be viewed as an application of the concept of model independence to the determination of subgrid model coefficients.

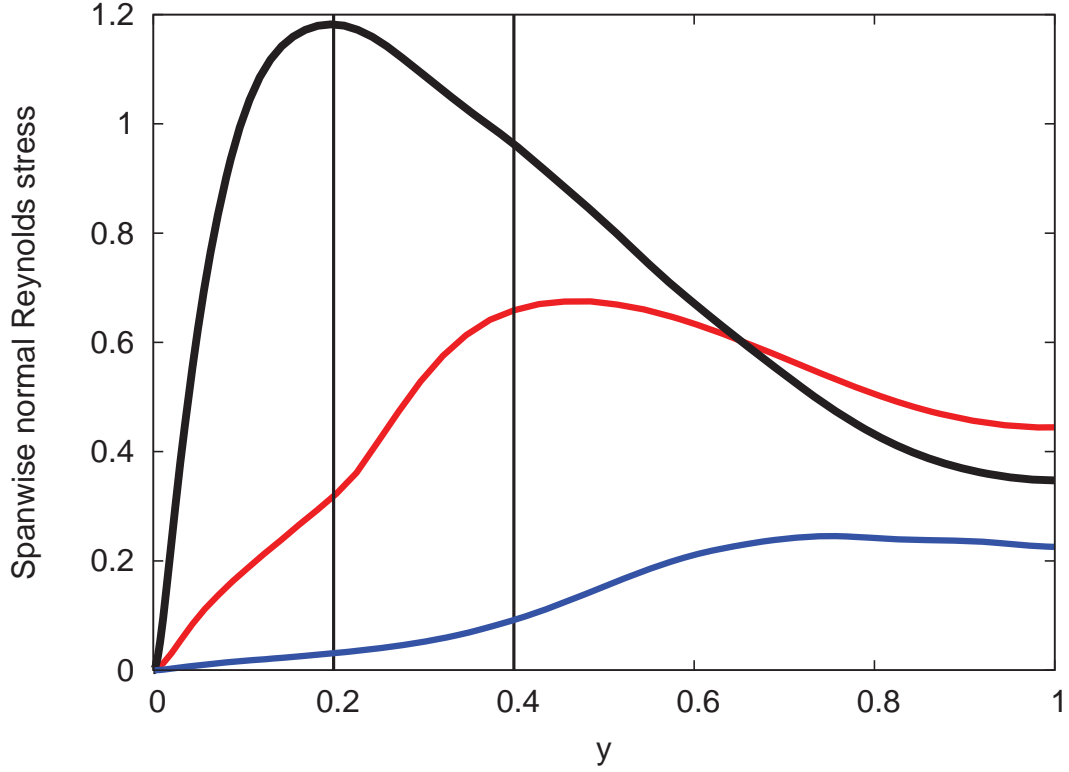


Figure 6. Normal resolved Reynolds-stress component from model-invariant computation (red curve), standard hybrid computation (blue curve) and DNS²³ (black curve) at $Re_\tau = 180$.

V. Conclusion

The analysis and computations presented in this paper show clearly that accurate results can hinge on dealing properly with the spurious effects of variations in the model blending parameter. Doing so provides a means of fully coupling the RANS and LES portions of the flow, with the benefits of improved physical fidelity and more freedom to place LES and RANS zones so the cost of LES need only be incurred where the flow physics dictates.

The present results demonstrate the ability of a model-invariant hybrid computation to give flow predictions significantly better than those of a standard hybrid computation. These predictions were insensitive to modelling artifacts such as transition-layer location and thickness and the shape of the blending function.

The success of these computations—using a relatively simple hybrid model and a crude approximation to the model sensitivities—is encouraging, but improvements will certainly be required as more complex flows are addressed. Formulating the concepts of a model-invariant hybrid computation independently of a specific hybrid model or a specific means of approximating the model sensitivities gives the widest possible latitude in developing improved hybrid models and model-sensitivity approximations. Creating these improved models within the model-invariant framework will, additionally, provide confidence that variations between the results of different models reflect true differences in physical fidelity and not differences due to spurious blending effects.

In addition to providing more freedom in the placement of LES/RANS transitions, further development of model-invariance concepts may have application to a number of related aspects of hybrid computations. Techniques for inflow turbulence generation, for example, might be aided by creating a RANS-to-LES transition at an inflow boundary, decreasing the fidelity and quantity of turbulence that must be generated. The close relationship between the blending parameter and grid resolution implies a natural relationship between

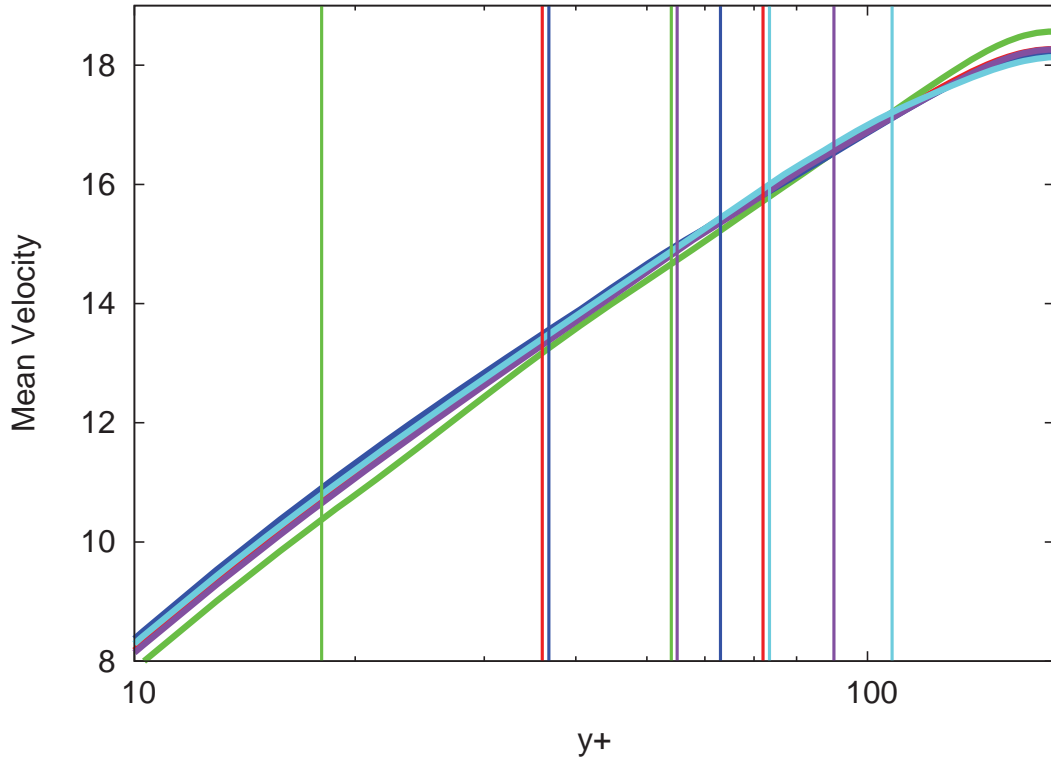


Figure 7. Mean velocity profiles from model-invariant computations with transition zones of various positions and thicknesses at $Re_\tau = 180$. Vertical lines represent edges of transition zones corresponding to profile of same color.

the model-invariant formulation and grid adaptation. Model sensitivities would be directly related to grid sensitivity to incorporate grid adaptation into the hybrid computation in a fundamental way. The blending parameter is distinct from the numerical grid resolution, however, and this provides an opportunity for a meaningful definition of grid convergence, in which numerical resolution would be increased while the blending parameter is unchanged. In general, the more precise picture the present formulation gives of hybrid computations should find a variety of uses.

Acknowledgments

Helpful comments by J.-R. Carlson, R. Baurle and W. Kleb are gratefully acknowledged. This work was funded by the Revolutionary Computational Aerosciences sub-project of the Aeronautical Sciences Project of NASA's Fundamental Aeronautics Program.

References

- ¹Travin, A., Shur, M., Strelets, M. and Spalart, P., "Detached-Eddy Simulations Past a Circular Cylinder," *Flow, Turbulence and Combustion*, Vol. 63, 1999, pp. 293–313.
- ²Nikitin, N. V., Nicoud, F., Wasistho, B., Squires, K. D. and Spalart, P. R., "An approach to wall modelling in large-eddy simulations," *Physics of Fluids*, Vol. 12, No. 7, 2000, pp. 1629–1632.
- ³Tucker, P. G. and Davidson, L., "Zonal $k - \ell$ based large eddy simulations," *Computers and Fluids*, Vol. 33, 2004, pp. 267–287.
- ⁴Keating, A., De Prisco, G. and Piomelli, U., "Interface conditions for hybrid RANS/LES calculations," *Int. J. Heat and Fluid Flow*, Vol. 27, 2006, pp. 777–788.
- ⁵Davidson, L. and Billson, M., "Hybrid LES-RANS using synthesized turbulent fluctuations for forcing in the interface

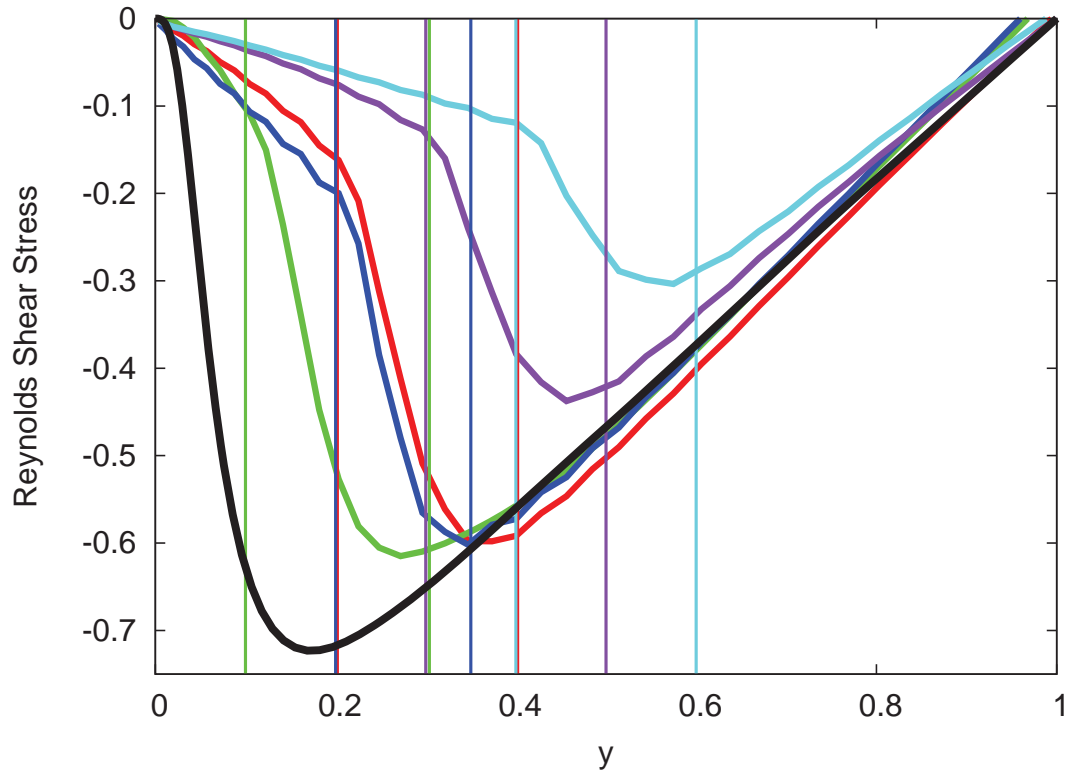


Figure 8. Resolved-flow contribution to Reynolds stress for various transition-zone positions and thicknesses at $Re_\tau = 180$. Vertical transition-zone edge lines color-coded to curves; black curve is DNS²³ turbulent stress.

region,” *Int. J. Heat and Fluid Flow*, Vol. 27, 2006, pp. 1028–1042.

⁶Hamba, F., “Log-layer mismatch and commutation error in hybrid RANS/LES simulation of channel flow,” *Int. J. Heat and Fluid Flow*, Vol. 30, 2009, pp. 20–31.

⁷Shur, M. L., Spalart, P. R., Strelets, M. Kh. and Travin, A., “A hybrid RANS-LES approach with delayed-DES and wall-modeled LES capabilities,” *Int. J. Heat and Fluid Flow*, Vol. 29, 2008, pp. 1638–1649.

⁸Choi, J.-I., Edwards, J. R. and Baurle, R. A., “Compressible Boundary Layer Predictions at High Reynolds Number using Hybrid LES/RANS Methods,” *AIAA J.*, Vol. 47, No. 9, 2009, pp. 2179–2193.

⁹Gieseking, D. A., Choi, J.-I., Edwards, J. R. and Hassan, H. A., “Simulation of Shock/Boundary Layer Interactions Using Improved LES/RANS Models,” *48th AIAA Aerospace Sciences Meeting*, January 4–7, 2010, Orlando, FL, AIAA-2010-111.

¹⁰Medic, G., Templeton, J. A. and Kalitzin, G., “A Formulation for Near-Wall RANS/LES Coupling,” *International Journal of Engineering Science*, Vol. 44, 2006, pp. 1099–1112.

¹¹Breuer, M., Jaffrezic, B. and Arora, K., “Hybrid LES-RANS Technique Based on a One-Equation Near-Wall Model,” *Theoretical and Computational Fluid Dynamics*, Vol. 22, 2008, pp. 157–187.

¹²Wallin, S. and Girimaji, S., “Commutation Error Mitigation in Variable-Resolution PANS Closure: Proof of Concept in Decaying Isotropic Turbulence,” *6th AIAA Theoretical Fluid Mechanics Conference*, June 27–30, 2011, Honolulu, HI, AIAA 2011-3105.

¹³Germano, M., “Properties of the Hybrid RANS/LES Filter,” *Theoretical and Computational Fluid Dynamics*, Vol. 17, 2004, 225–231.

¹⁴Rajamani, B. and Kim, J., “A Hybrid-Filter Approach to Turbulence Simulation,” *Flow Turbulence Combust.*, Vol. 85, 2010, pp. 421–441.

¹⁵Sanchez-Rocha, M. and Menon, S., “The Compressible Hybrid RANS/LES Formulation Using an Additive Operator,” *Journal of Computational Physics*, Vol. 228, 2009, pp. 2037–2062.

¹⁶Sanchez-Rocha, M. and Menon, S., “An Order-of-Magnitude Approximation for the Hybrid Terms in the Compressible Hybrid RANS/LES Governing Equations,” *Journal of Turbulence*, Vol. 12, 2011, N16.

¹⁷Woodruff, S. L., “Coupling Turbulence in Hybrid LES-RANS Techniques,” *Seventh International Symposium on Turbulence and Shear-Flow Phenomena*, Ottawa, Canada, July 28–31, 2010.

¹⁸Hamba, F., “Analysis of filtered Navier-Stokes equation for hybrid RANS/LES simulation,” *Physics of Fluids*, Vol. 23, 2011, 015108.

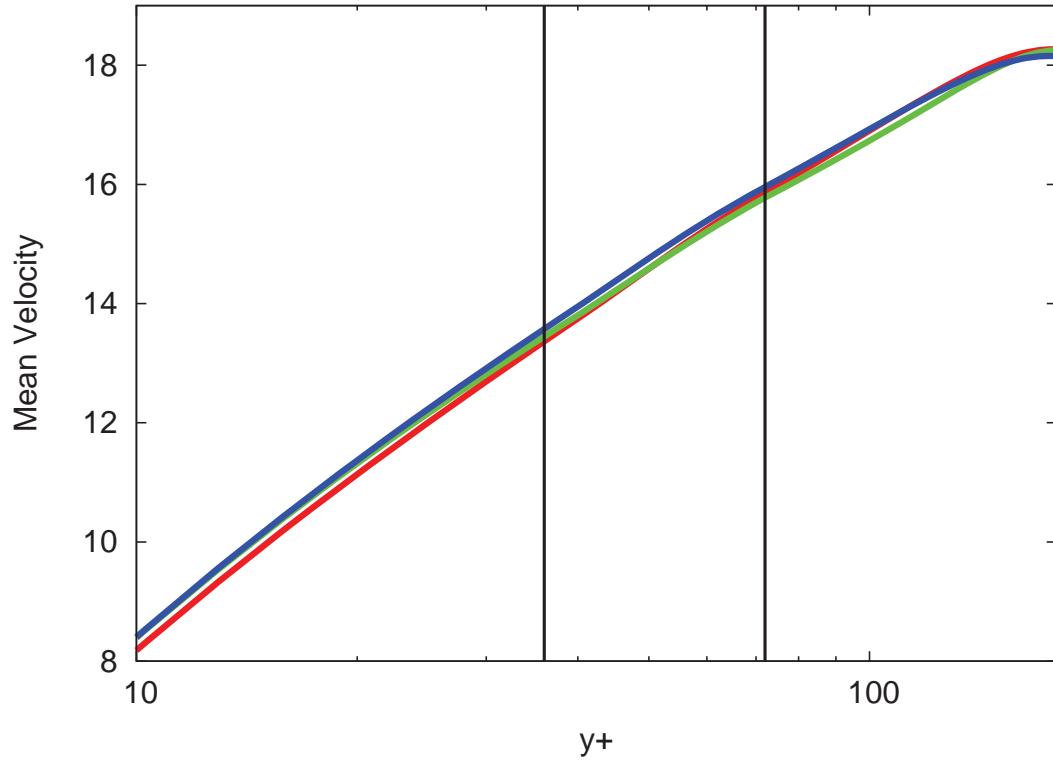


Figure 9. Mean-velocity profiles for various blending-function shapes at $Re_\tau = 180$: spline (red curve), linear (green curve), hyperbolic tangent (blue curve).

¹⁹Speziale, C. G., “Turbulence Modeling for Time-Dependent RANS and VLES: A Review” *AIAA J.*, Vol. 36, No. 2, 1998, pp. 173–184.

²⁰Spalart, P. R., “Detached-Eddy Simulation,” *Annual Review of Fluid Mechanics*, Vol. 41, 2009, pp. 181–202.

²¹Strelets, M., “Detached Eddy Simulation of Massively Separated Flows,” *39th AIAA Aerospace Sciences Meeting*, January 8–11, 2001, Reno, NV, AIAA-2001-0879.

²²Menter, F. R., “Two-Equation Eddy-Viscosity Turbulence Models for Engineering Applications,” *AIAA J.*, Vol. 32, No. 8, 1994, pp. 1598–1605.

²³Moser, R., Kim, J. and Mansour, N., “DNS of Turbulent Channel Flow up to $Re_\tau = 590$,” *Physics of Fluids*, Vol. 11, No. 4, 1999, pp. 943–945.

²⁴CFL3D Version V Manual, <http://cfl3d.larc.nasa.gov>, last accessed April 30, 2013.

²⁵Germano, M., “Turbulence: the filtering approach,” *Journal of Fluid Mechanics*, Vol. 238, 1992, pp. 325–336.

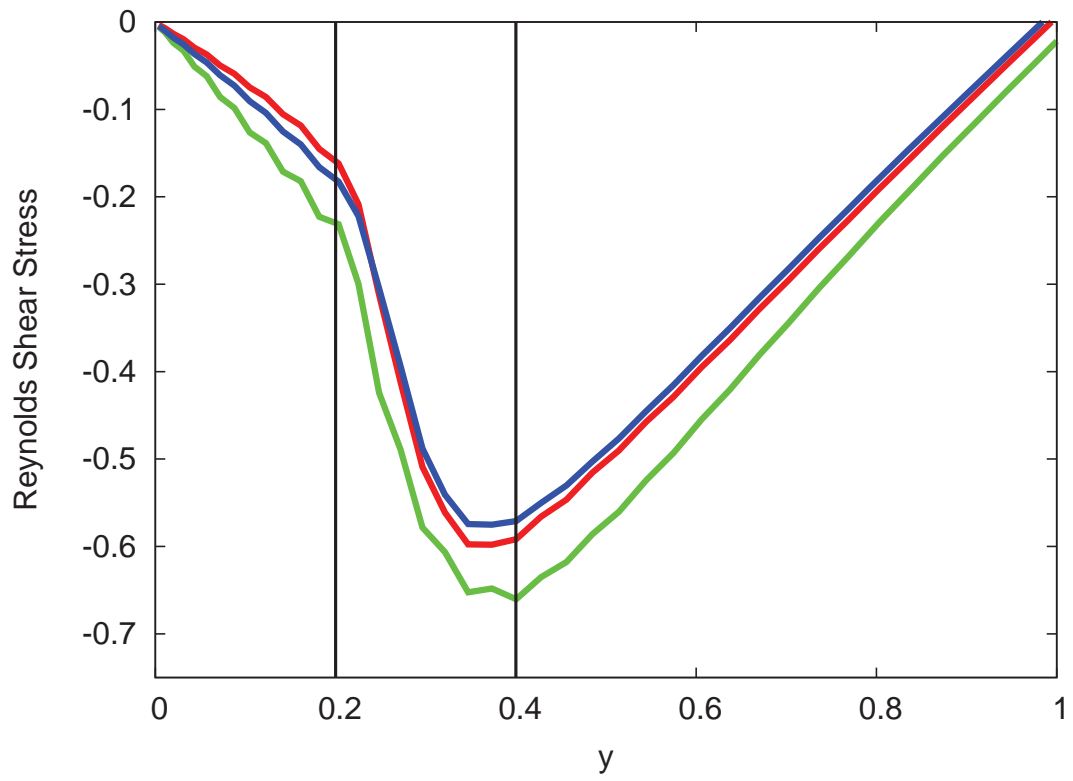


Figure 10. Resolved shear-stress profiles for various blending-function shapes at $Re_\tau = 180$: spline (red curve), linear (green curve), hyperbolic tangent (blue curve).

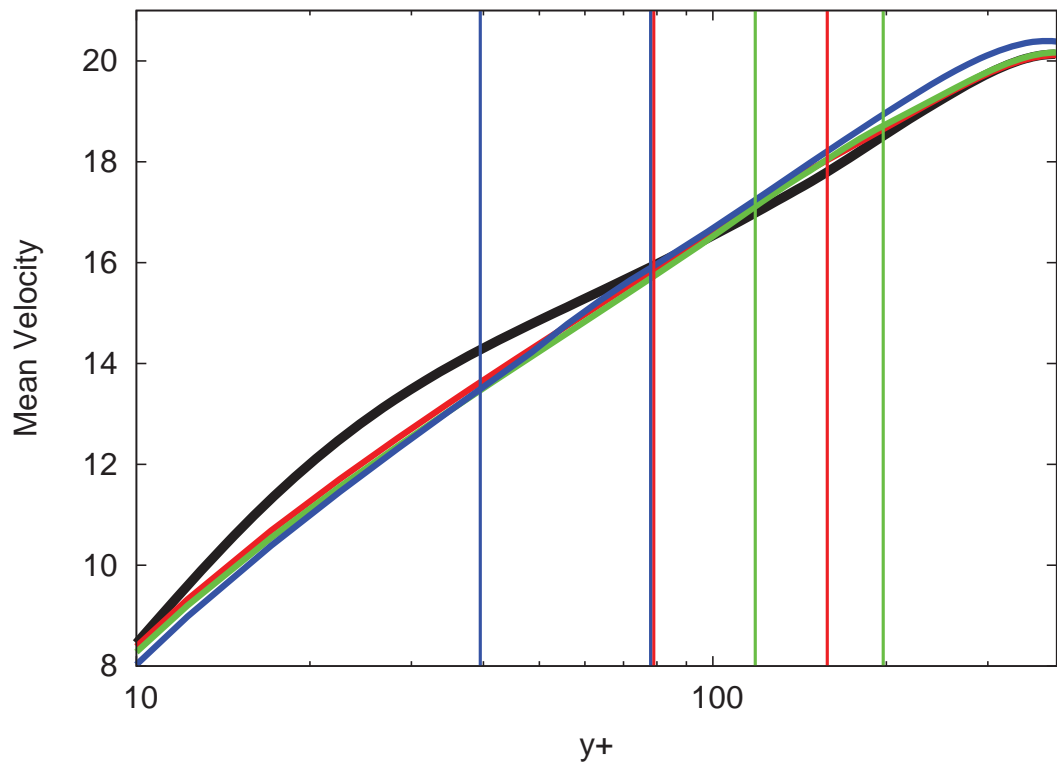


Figure 11. Mean-velocity profiles for various transition-zone positions and thicknesses at $Re_\tau = 395$. Curves color-coded to vertical lines representing edges of transition zones; black curve is DNS.²³

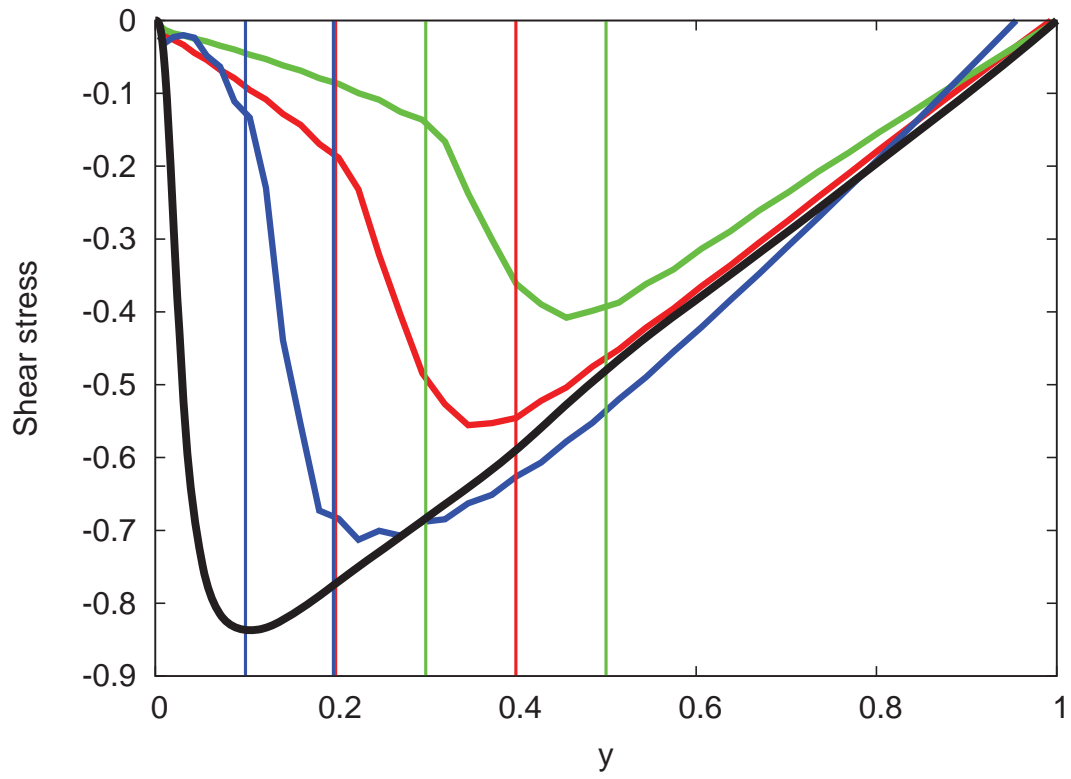


Figure 12. Resolved shear-stress profiles for various transition-zone positions and thicknesses at $Re_\tau = 395$. Curves color-coded to vertical lines representing edges of transition zones; black curve is DNS.²³